Supplementary Information for

Uncovering the genetic blueprint of the *C. elegans* nervous system

István A. Kovács, Dániel L. Barabási, and Albert-László Barabási

Albert-László Barabási.
E-mail: a.barabasi@northeastern.edu

This PDF file includes:

Supplementary text
Figs. S1 to S6
SI References

Supporting Information Text

Available Connectomes. The neural system of *C. elegans* consists of chemical synapses and gap junctions between 302 neurons. Graph theoretical analyses of *C. elegans* connectomes typically restrict the circuit to the connected somatic nervous system of 279 neurons, excluding 20 neurons in pharyngeal nervous system and 3 somatic neurons (CANL/R and VC06) that, in the Varshney et al. reconstruction (1), do not synapse with other neurons. We studied two different reconstructions:

- **Cook et al.** reconstructs a gap junction network with 1,051 undirected links, including 11 self-loops (2).

- **Varshney et al.** provides a more conservative reconstruction, resulting in a gap junction network of 517 links, of which 3 are self-loops (1).

Given its updated methodology, the Cook et al. connectome is utilized in the body of the paper. However, we also performed the SCM analysis on the Varshney connectome (SI Appendix, Figure S4), which resulted in 12 significant interactions that were shared with the Cook et al. analysis: (1) inx-3–inx-3, (2) inx-9–inx-17 , (3) inx-19–inx-19, (4) unc-9–unc-9, (5) inx-9–inx-9, (6) inx-13–inx-13, (7) inx-12–inx-12, (8) inx-2–inx-10, (9) inx-6–inx-18, (10) inx-7–inx-7, (11) inx-8–inx-12, and (12) che-7–inx-17.

Heteromeric Gap Junctions. As documented in vertebrate connexins, two or more innexins might form mixed, heteromeric hemi-channels, playing an important role in building the connectome. Therefore, innexins are also expected to form heteromeric GJs (3), meaning that in a given neuron the expression of two (or more) innexins are required to establish a GJ with another neuron (4). Heteromeric hemi-channels formed by two kinds of innexin proteins can be incorporated in our model by adding the joint (logical AND) expression of innexin pairs to X as additional labels. In general, at the pairwise level, such a step increases the dimensionality of the problem by an order of magnitude (from 18 to 171 labels) for X and from 171 potential rules to $14,706$ rules in O. In practice, the complexity of the problem might reduce if some of the combinatorial labels result in already existing patterns or no expression. Yet, data incompleteness and noise in single gene expression might render computational estimates of combinatorial expression highly unreliable. To avoid false positives, the inference of heteromeric rules is left as future work, gaining more relevance once the homomeric rules have been experimentally validated.

Chemical Synapses. Given that the formation of GJs is governed by innexin expression, we know the genetic basis in which the rules operate. To perform the same analyses for chemical synapses, we must extend the search basis to a much larger set of genes, including any gene that could contribute to the identity of the neurons and impact synapse formation. Unless the correct biological basis can be further restricted, we lack the labels corresponding to the combination of proteins contributing to synapse formation. One way to reduce the dimensionality of the problem is to focus on transcription factor (TF) expression only. However, as opposed to innexin expression, adult TF expression might not be strongly related to the expression history during development, shaping the chemical synapses. Ideally, we would need to restrict the number of combinatorial labels considered to the number of neurons or less, to reliably infer the chemical rules. However, even then, given that synapses are directed, we need two sets of labels, one for identifying the input neurons (X) and one for the output neurons (Y), extending the Connectome Model into a Directed Connectome Model (DCM)

$$B = XOY \ . \tag{1}$$

The DCM can be solved similarly to the CM as $\tilde{O} = X^+ B Y^+$. While the DCM can also incorporate spatial constraints, to assess statistical significance, the directed extension of the subgraph randomization protocol is needed.

Spectral Interpretation of the Wiring Rules. A positive definite O would mean that the genetic rules can be captured by abstract, yet simple, positive rules in the diagonal basis, where synapses are formed due to independent rules, solely on the basis of genetic feature similarity. On the contrary, the existence of at least one negative eigenvalue indicates that the nervous system is not only wired based on (abstract) genetic similarity, but also based on genetic dissimilarity, i.e. some kind of complementarity between different genetic features. Let's illustrate this for a single genetic rule. A single inx-2–inx-2 self-interaction would be a positive diagonal rule, where GJs are formed when two neurons both express inx-2, showcasing expression profile similarity. In contrast, a single wiring rule inx-2–inx-3 leads to both a positive and a negative eigenvalue, where similar neurons do not necessarily interact, but need complementary expression, i.e. the expression of inx-2 in one neuron and inx-3 in the other, for GJ formation.

From the solution of Eq. (5) we find that in *C. elegans*, the genetic rule matrix, O, has at least four negative eigenvalues (SI Appendix, Figure S4). The presence of negative eigenvalues of O indicate that genetic similarity and complementarity together drive GJ formation. Note, that we could not have arrived to this conclusion by directly inspecting the spectrum of the connectome B, given that B is truncated by spatial constraints (C).

István A. Kovács, Dániel L. Barabási, and Albert-László Barabási
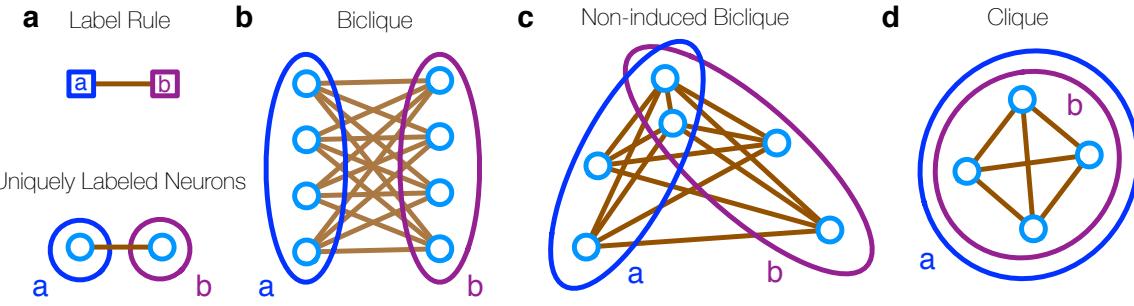
Fig. S1. Topologies resulting from a single, deterministic rule. A genetic rule, connecting two labels, can appear very differently in the connectome depending on the distribution of the labels in the network. Each rule O_{ab} linking two labels (a and b) is expected to encode $E_{ab} = O_{ab} (N_a N_b - N_{ab}(N_{ab} - 1)/2)$ neural connections, where N_a and N_b are the number of neurons with labels a and b, and N_{ab} is the number of neurons expressing both labels. **a)** A rule can correspond to a single neural connection if the labels identify individual neurons. **b)** If the labels extend over multiple neurons but share no common neurons, we have a biclique in the graph. **c)** If the labels overlap for some neurons, we observe a generalized, non-induced biclique, reminiscent of core-periphery structure. **d)** If the labels overlap completely, a clique is formed. Note, that in general the rules are weighted, leading to subgraphs of the structures above.
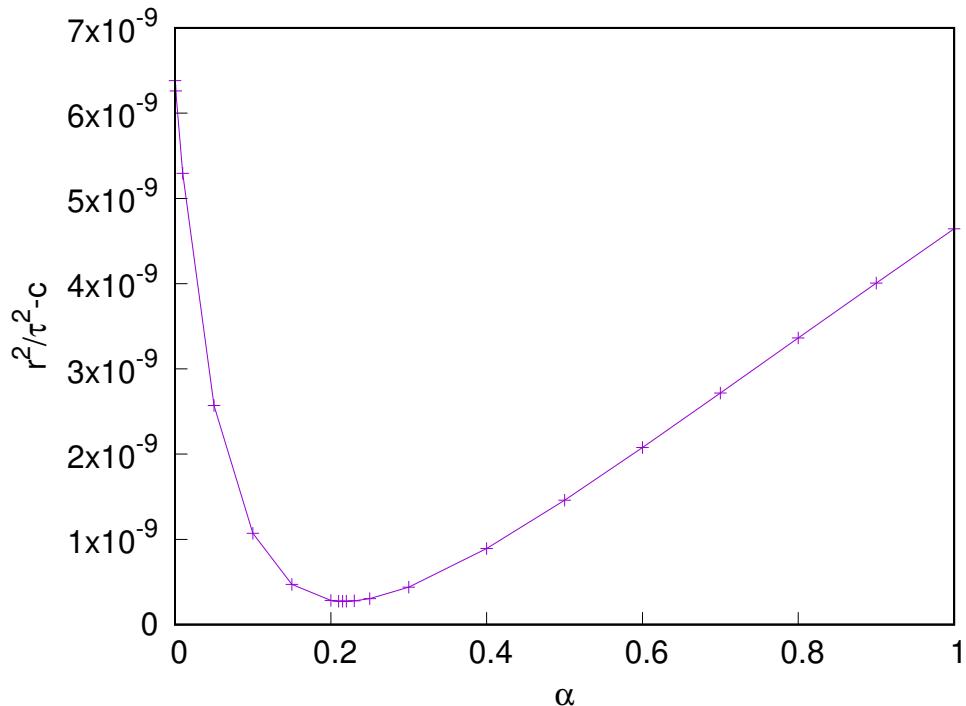
Fig. S2. The optimal $\alpha = 0.215$ regularization parameter for the SCM. The y-axis shows the r^2/τ^2 value above a constant background of $c = 8.55 \times 10^{-6}$. Here we show the results for the Cook et al. data.

|	inx-1	inx-10	inx-11	inx-12	inx-13	inx-17	inx-18	inx-19	inx-2	inx-3	inx-5	inx-6	inx-7	inx-8	inx-9	che-7	unc-7	unc-9
inx-1	-0.07	0.14	0.29	-0.11	-0.35	0.09	0.15	0.04	-0.12	-0.24	0.29	0.18	0.13	-0.35	0.01	0.14	0.08	-0.01
inx-10	0.14	0.42	0.78	0.31	-0.72	0.36	-0.46	0.16	0.66	0.75	0.78	-0.18	0.08	0.38	-0.33	-0.13	-0.04	0.08
inx-11	0.29	0.78	0.00	0.25	-0.22	-0.31	-0.32	-0.09	-0.01	0.43	0.00	0.04	-0.06	-0.01	-0.01	-0.03	-0.10	-0.02
inx-12	-0.11	0.31	0.25	0.38	0.14	-0.23	0.01	0.09	-0.37	0.04	0.25	0.00	0.01	0.26	-0.38	-0.02	0.05	-0.03
inx-13	-0.35	-0.72	-0.22	0.14	0.22	0.52	0.12	-0.01	-0.68	-0.13	-0.22	0.02	0.16	0.32	-0.24	-0.09	0.05	-0.04
inx-17	0.09	0.36	-0.31	-0.23	0.52	-0.02	0.00	0.11	-0.33	-0.29	-0.31	-0.06	-0.16	-0.09	0.33	0.26	-0.02	-0.02
inx-18	0.15	-0.46	-0.32	0.01	0.12	0.00	0.12	-0.07	0.40	0.13	-0.32	0.22	0.00	-0.15	-0.09	-0.06	0.03	0.03
inx-19	0.04	0.16	-0.09	0.09	-0.01	0.11	-0.07	0.14	-0.10	0.03	-0.09	-0.01	-0.03	0.01	0.03	0.08	-0.01	-0.04
inx-2	-0.12	0.66	-0.01	-0.37	-0.68	-0.33	0.40	-0.10	0.78	0.31	-0.01	-0.22	-0.31	0.00	0.18	0.23	-0.01	0.05
inx-3	-0.24	0.75	0.43	0.04	-0.13	-0.29	0.13	0.03	0.31	0.25	0.43	-0.20	-0.03	0.02	-0.02	-0.07	-0.05	0.03
inx-5	0.29	0.78	0.00	0.25	-0.22	-0.31	-0.32	-0.09	-0.01	0.43	0.00	0.04	-0.06	-0.01	-0.01	-0.03	-0.10	-0.02
inx-6	0.18	-0.18	0.04	0.00	0.02	-0.06	0.22	-0.01	-0.22	-0.20	0.04	0.28	0.07	0.01	-0.28	0.08	0.01	0.03
inx-7	0.13	0.08	-0.06	0.01	0.16	-0.16	0.00	-0.03	-0.31	-0.03	-0.06	0.07	0.09	0.14	-0.04	0.04	0.06	-0.05
inx-8	-0.35	0.38	-0.01	0.26	0.32	-0.09	-0.15	0.01	0.00	0.02	-0.01	0.01	0.14	0.08	-0.33	-0.02	-0.02	-0.02
inx-9	0.01	-0.33	-0.01	-0.38	-0.24	0.33	-0.09	0.03	0.18	-0.02	-0.01	-0.28	-0.04	-0.33	0.64	-0.10	-0.04	0.06
che-7	0.14	-0.13	-0.03	-0.02	-0.09	0.26	-0.06	0.08	0.23	-0.07	-0.03	0.08	0.04	-0.02	-0.10	0.04	0.01	0.03
unc-7	0.08	-0.04	-0.10	0.05	0.05	-0.02	0.03	-0.01	-0.01	-0.05	-0.10	0.01	0.06	-0.02	-0.04	0.01	0.07	-0.01
unc-9	-0.01	0.08	-0.02	-0.03	-0.04	-0.02	0.03	-0.04	0.05	0.03	-0.02	0.03	-0.05	-0.02	0.06	0.03	-0.01	0.06

	inx-1	inx-10	inx-11	inx-12	inx-13	inx-17	inx-18	inx-19	inx-2	inx-3	inx-5	inx-6	inx-7	inx-8	inx-9	che-7	unc-7	unc-9
inx-1	-0.6	-0.2	1.7	-1.2	-1.0	0.1	2.0	-0.4	-1.0	-1.4	1.7	0.7	0.9	-1.0	0.3	0.8	0.3	-0.2
inx-10	-0.2	1.8	3.0	0.8	-3.4	0.0	-1.6	0.0	2.1	3.4	3.0	-1.2	0.0	1.1	-1.2	-2.2	-1.1	0.9
inx-11	1.7	3.0	-	2.0	-0.6	-1.7	-2.5	-0.9	-0.6	1.4	-	0.6	-0.3	-0.6	-0.6	-0.4	-1.0	-0.5
inx-12	-1.2	0.8	2.0	5.6	1.5	-1.8	0.0	0.7	-1.4	0.3	2.0	0.2	-1.4	2.6	-3.8	-0.7	0.8	-0.9
inx-13	-1.0	-3.4	-0.6	1.5	2.4	2.4	0.7	-0.4	-1.3	-1.5	-0.6	0.2	2.0	2.8	-2.2	-1.0	1.3	-0.8
inx-17	0.1	0.0	-1.7	-1.8	2.4	0.5	0.4	1.7	-1.6	-1.7	-1.7	-0.4	-0.9	-0.2	2.5	2.8	0.8	-0.7
inx-18	2.0	-1.6	-2.5	0.0	0.7	0.4	1.9	-1.2	1.7	0.7	-2.5	2.4	0.9	-1.8	-0.7	-0.8	0.5	0.4
inx-19	-0.4	0.0	-0.9	0.7	-0.4	1.7	-1.2	3.4	0.3	1.0	-0.9	-0.8	-1.7	-0.9	1.5	1.1	-0.8	-1.8
inx-2	-1.0	2.1	-0.6	-1.4	-1.3	-1.6	1.7	0.3	1.6	0.9	-0.6	-1.0	-1.5	0.0	0.7	1.7	0.4	0.1
inx-3	-1.4	3.4	1.4	0.3	-1.5	-1.7	0.7	1.0	0.9	2.8	1.4	-1.8	-0.9	0.2	-0.2	-1.1	-1.9	1.0
inx-5	1.7	3.0	-	2.0	-0.6	-1.7	-2.5	-0.9	-0.6	1.4	-	0.6	-0.3	-0.6	-0.6	-0.4	-1.0	-0.5
inx-6	0.7	-1.2	0.6	0.2	0.2	-0.4	2.4	-0.8	-1.0	-1.8	0.6	2.5	0.6	-0.1	-2.6	0.9	-0.2	0.6
inx-7	0.9	0.0	-0.3	-1.4	2.0	-0.9	0.9	-1.7	-1.5	-0.9	-0.3	0.6	2.4	1.8	0.3	0.8	1.7	-2.5
inx-8	-1.0	1.1	-0.6	2.6	2.8	-0.2	-1.8	-0.9	0.0	0.2	-0.6	-0.1	1.8	0.6	-2.8	-0.6	-1.3	-0.3
inx-9	0.3	-1.2	-0.6	-3.8	-2.2	2.5	-0.7	1.5	0.7	-0.2	-0.6	-2.6	0.3	-2.8	5.0	-1.4	-0.5	1.4
che-7	0.8	-2.2	-0.4	-0.7	-1.0	2.8	-0.8	1.1	1.7	-1.1	-0.4	0.9	0.8	-0.6	-1.4	0.3	-0.4	0.8
unc-7	0.3	-1.1	-1.0	0.8	1.3	0.8	0.5	-0.8	0.4	-1.9	-1.0	-0.2	1.7	-1.3	-0.5	-0.4	1.2	-1.7
unc-9	-0.2	0.9	-0.5	-0.9	-0.8	-0.7	0.4	-1.8	0.1	1.0	-0.5	0.6	-2.5	-0.3	1.4	0.8	-1.7	3.1

Fig. S3. Solution of the SCM for Cook et al. data. Top: Positive rule weights are indicated in red while negative rules in blue. Bottom: The corresponding z-scores.

István A. Kovács, Dániel L. Barabási, and Albert-László Barabási

	inx-1	inx-10	inx-11	inx-12	inx-13	inx-17	inx-18	inx-19	inx-2	inx-3	inx-5	inx-6	inx-7	inx-8	inx-9	che-7	unc-7	unc-9
inx-1	0.12	-0.25	0.43	0.00	-0.30	0.36	0.09	-0.01	0.00	0.03	0.43	0.15	0.09	-0.35	0.02	0.14	0.05	-0.08
inx-10	-0.25	0.21	0.42	-0.05	-0.37	0.26	-0.16	0.08	0.73	0.23	0.42	0.06	0.01	0.05	0.10	-0.07	-0.04	0.05
inx-11	0.43	0.42	0.00	0.20	-0.37	-0.29	-0.29	-0.05	0.01	0.46	0.00	-0.06	-0.04	0.01	0.01	-0.09	-0.03	0.01
inx-12	0.00	-0.05	0.20	0.37	0.12	-0.08	-0.04	0.04	-0.22	0.05	0.20	0.00	-0.02	0.13	-0.33	-0.04	0.01	0.00
inx-13	-0.30	-0.37	-0.37	0.12	0.38	0.02	0.23	-0.01	-0.85	-0.19	-0.37	0.02	0.09	0.14	-0.22	-0.01	0.06	-0.07
inx-17	0.36	0.26	-0.29	-0.08	0.02	0.06	-0.15	0.05	-0.09	-0.14	-0.29	-0.11	-0.14	-0.03	0.30	0.23	-0.05	0.03
inx-18	0.09	-0.16	-0.29	-0.04	0.23	-0.15	0.11	-0.04	-0.08	-0.05	-0.29	0.12	0.03	-0.01	-0.05	-0.03	0.06	-0.04
inx-19	-0.01	0.08	-0.05	0.04	-0.01	0.05	-0.04	0.09	0.01	0.03	-0.05	-0.03	-0.03	-0.03	0.01	0.04	0.01	-0.01
inx-2	0.00	0.73	0.01	-0.22	-0.85	-0.09	-0.08	0.01	1.14	0.37	0.01	-0.03	-0.28	0.01	0.04	0.22	0.02	0.16
inx-3	0.03	0.23	0.46	0.05	-0.19	-0.14	-0.05	0.03	0.37	0.45	0.46	-0.11	-0.14	0.00	-0.10	-0.09	-0.04	0.04
inx-5	0.43	0.42	0.00	0.20	-0.37	-0.29	-0.29	-0.05	0.01	0.46	0.00	-0.06	-0.04	0.01	0.01	-0.09	-0.03	0.01
inx-6	0.15	0.06	-0.06	0.00	0.02	-0.11	0.12	-0.03	-0.03	-0.11	-0.06	0.08	0.00	0.02	-0.10	0.13	-0.01	0.01
inx-7	0.09	0.01	-0.04	-0.02	0.09	-0.14	0.03	-0.03	-0.28	-0.14	-0.04	0.00	0.10	0.06	0.02	0.03	0.05	-0.05
inx-8	-0.35	0.05	0.01	0.13	0.14	-0.03	-0.01	-0.03	0.01	0.00	0.01	0.02	0.06	0.07	-0.17	-0.01	-0.02	0.00
inx-9	0.02	0.10	0.01	-0.33	-0.22	0.30	-0.05	0.01	0.04	-0.10	0.01	-0.10	0.02	-0.17	0.46	-0.02	-0.02	0.01
che-7	0.14	-0.07	-0.09	-0.04	-0.01	0.23	-0.03	0.04	0.22	-0.09	-0.09	0.13	0.03	-0.01	-0.02	0.06	0.00	0.00
unc-7	0.05	-0.04	-0.03	0.01	0.06	-0.05	0.06	0.01	0.02	-0.04	-0.03	-0.01	0.05	-0.02	-0.02	0.00	0.04	-0.03
unc-9	-0.08	0.05	0.01	0.00	-0.07	0.03	-0.04	-0.01	0.16	0.04	0.01	0.01	-0.05	0.00	0.01	0.00	-0.03	0.07

	inx-1	inx-10	inx-11	inx-12	inx-13	inx-17	inx-18	inx-19	inx-2	inx-3	inx-5	inx-6	inx-7	inx-8	inx-9	che-7	unc-7	unc-9
inx-1	1.3	-1.7	3.0	-0.4	-1.8	2.5	1.4	-0.7	-0.7	0.7	3.0	1.1	1.0	-2.1	0.5	1.8	0.6	-2.1
inx-10	-1.7	1.5	1.8	-0.8	-2.5	0.8	-1.0	0.5	2.2	1.7	1.8	0.4	-0.3	0.0	0.8	-1.4	-1.1	1.1
inx-11	3.0	1.8	-	2.0	-1.9	-1.8	-2.5	-0.8	-0.2	1.8	-	-0.3	0.0	-0.2	-0.2	-1.2	-0.4	-0.3
inx-12	-0.4	-0.8	2.0	7.0	2.0	-0.7	-1.0	0.4	-1.3	1.0	2.0	-0.3	-1.1	2.0	-4.9	-1.7	-0.5	0.2
inx-13	-1.8	-2.5	-1.9	2.0	4.4	0.2	2.8	-0.6	-2.6	-2.3	-1.9	0.0	1.6	1.7	-2.9	-0.1	1.8	-2.0
inx-17	2.5	0.8	-1.8	-0.7	0.2	0.5	-1.8	1.6	-0.8	-1.1	-1.8	-1.0	-1.6	0.3	2.6	3.2	-0.4	-0.1
inx-18	1.4	-1.0	-2.5	-1.0	2.8	-1.8	2.8	-1.1	0.0	-1.6	-2.5	2.2	1.3	0.0	-0.6	-0.4	2.2	-1.6
inx-19	-0.7	0.5	-0.8	0.4	-0.6	1.6	-1.1	4.5	0.6	1.5	-0.8	-1.2	-2.2	-1.8	0.8	0.8	0.2	-1.0
inx-2	-0.7	2.2	-0.2	-1.3	-2.6	-0.8	0.0	0.6	2.4	1.7	-0.2	-0.6	-1.8	-0.2	0.5	1.3	0.3	1.1
inx-3	0.7	1.7	1.8	1.0	-2.3	-1.1	-1.6	1.5	1.7	6.5	1.8	-1.6	-3.1	-0.1	-1.6	-1.9	-1.3	1.7
inx-5	3.0	1.8	-	2.0	-1.9	-1.8	-2.5	-0.8	-0.2	1.8	-	-0.3	0.0	-0.2	-0.2	-1.2	-0.4	-0.3
inx-6	1.1	0.4	-0.3	-0.3	0.0	-1.0	2.2	-1.2	-0.6	-1.6	-0.3	1.1	0.0	0.4	-0.9	2.8	-0.7	0.0
inx-7	1.0	-0.3	0.0	-1.1	1.6	-1.6	1.3	-2.2	-1.8	-3.1	0.0	0.0	3.8	1.3	0.8	0.2	1.9	-2.2
inx-8	-2.1	0.0	-0.2	2.0	1.7	0.3	0.0	-1.8	-0.2	-0.1	-0.2	0.4	1.3	0.9	-2.3	-0.3	-1.2	0.5
inx-9	0.5	0.8	-0.2	-4.9	-2.9	2.6	-0.6	0.8	0.5	-1.6	-0.2	-0.9	0.8	-2.3	5.5	0.0	0.1	0.1
che-7	1.8	-1.4	-1.2	-1.7	-0.1	3.2	-0.4	0.8	1.3	-1.9	-1.2	2.8	0.2	-0.3	0.0	1.7	-0.4	-0.5
unc-7	0.6	-1.1	-0.4	-0.5	1.8	-0.4	2.2	0.2	0.3	-1.3	-0.4	-0.7	1.9	-1.2	0.1	-0.4	1.4	-2.6
unc-9	-2.1	1.1	-0.3	0.2	-2.0	-0.1	-1.6	-1.0	1.1	1.7	-0.3	0.0	-2.2	0.5	0.1	-0.5	-2.6	4.6

Fig. S4. Solution of the SCM for Varshney et al. data. Top: Positive rule weights are indicated in red while negative rules in blue at the optimal $\alpha = 0.12$ regularization parameter value. Bottom: The corresponding z-scores.
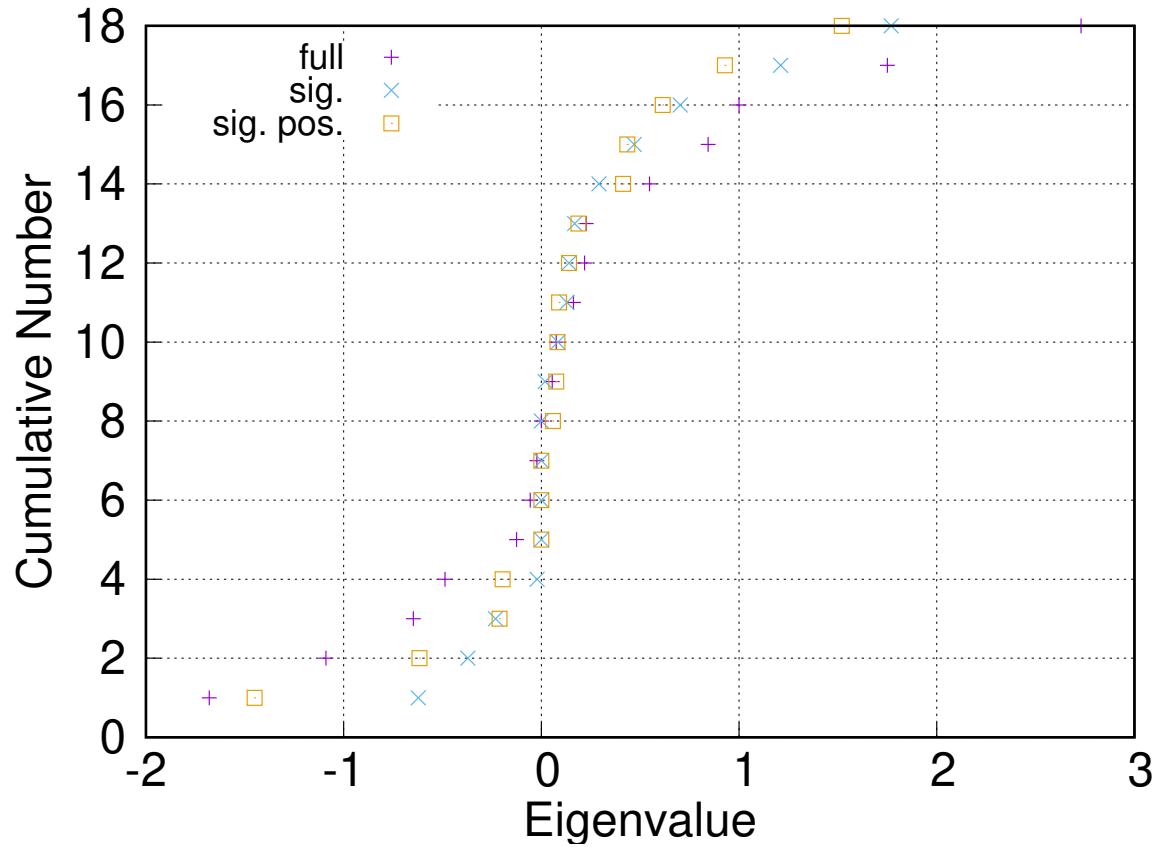
Fig. S5. Eigenvalues of O**.** The obtained genetic rules have an indefinite spectrum as shown for the obtained O matrix, keeping all entries (full), only the significant ones with $|z| \geq 2$ (sig.) or only the significant positive entries (sig. pos.).

István A. Kovács, Dániel L. Barabási, and Albert-László Barabási

	inx-1	inx-10	inx-11	inx-12	inx-13	inx-17	inx-18	inx-19	inx-2	inx-3	inx-5	inx-6	inx-7	inx-8	inx-9	che-7	unc-7	unc-9
inx-1	-0.07	0.16	0.34	-0.10	-0.40	0.10	0.15	0.04	-0.10	-0.22	0.34	0.18	0.12	-0.37	-0.01	0.13	0.08	-0.01
inx-10	0.16	0.45	1.15	0.37	-0.86	0.43	-0.59	0.19	1.10	0.89	1.15	-0.26	0.05	0.39	-0.50	-0.17	-0.04	0.10
inx-11	0.34	1.15	0.00	0.29	-0.60	-0.68	-0.55	-0.10	0.13	1.02	0.00	0.02	-0.16	0.13	0.13	-0.02	-0.13	0.02
inx-12	-0.10	0.37	0.29	0.40	0.11	-0.27	0.00	0.10	-0.40	0.06	0.29	0.00	0.00	0.28	-0.41	-0.02	0.04	-0.03
inx-13	-0.40	-0.86	-0.60	0.11	0.24	0.67	0.15	-0.01	-0.99	-0.20	-0.60	0.06	0.19	0.34	-0.20	-0.09	0.06	-0.06
inx-17	0.10	0.43	-0.68	-0.27	0.67	0.00	0.05	0.10	-0.69	-0.45	-0.68	-0.02	-0.14	-0.10	0.49	0.29	-0.02	-0.03
inx-18	0.15	-0.59	-0.55	0.00	0.15	0.05	0.14	-0.08	0.40	0.10	-0.55	0.23	0.01	-0.17	-0.07	-0.06	0.03	0.02
inx-19	0.04	0.19	-0.10	0.10	-0.01	0.10	-0.08	0.14	-0.12	0.03	-0.10	-0.01	-0.04	0.02	0.03	0.08	-0.01	-0.03
inx-2	-0.10	1.10	0.13	-0.40	-0.99	-0.69	0.40	-0.12	1.53	0.68	0.13	-0.42	-0.42	-0.07	0.09	0.22	-0.04	0.12
inx-3	-0.22	0.89	1.02	0.06	-0.20	-0.45	0.10	0.03	0.68	0.37	1.02	-0.25	-0.08	0.03	-0.10	-0.08	-0.06	0.06
inx-5	0.34	1.15	0.00	0.29	-0.60	-0.68	-0.55	-0.10	0.13	1.02	0.00	0.02	-0.16	0.13	0.13	-0.02	-0.13	0.02
inx-6	0.18	-0.26	0.02	0.00	0.06	-0.02	0.23	-0.01	-0.42	-0.25	0.02	0.33	0.09	0.02	-0.27	0.08	0.02	0.02
inx-7	0.12	0.05	-0.16	0.00	0.19	-0.14	0.01	-0.04	-0.42	-0.08	-0.16	0.09	0.10	0.14	-0.01	0.04	0.07	-0.06
inx-8	-0.37	0.39	0.13	0.28	0.34	-0.10	-0.17	0.02	-0.07	0.03	0.13	0.02	0.14	0.10	-0.35	-0.03	-0.02	-0.02
inx-9	-0.01	-0.50	0.13	-0.41	-0.20	0.49	-0.07	0.03	0.09	-0.10	0.13	-0.27	-0.01	-0.35	0.72	-0.09	-0.03	0.04
che-7	0.13	-0.17	-0.02	-0.02	-0.09	0.29	-0.06	0.08	0.22	-0.08	-0.02	0.08	0.04	-0.03	-0.09	0.04	0.01	0.03
unc-7	0.08	-0.04	-0.13	0.04	0.06	-0.02	0.03	-0.01	-0.04	-0.06	-0.13	0.02	0.07	-0.02	-0.03	0.01	0.07	-0.01
unc-9	-0.01	0.10	0.02	-0.03	-0.06	-0.03	0.02	-0.03	0.12	0.06	0.02	0.02	-0.06	-0.02	0.04	0.03	-0.01	0.06

	inx-1	inx-10	inx-11	inx-12	inx-13	inx-17	inx-18	inx-19	inx-2	inx-3	inx-5	inx-6	inx-7	inx-8	inx-9	che-7	unc-7	unc-9
inx-1	0.12	-0.26	0.47	0.01	-0.34	0.37	0.08	-0.01	0.07	0.05	0.47	0.15	0.09	-0.37	0.00	0.14	0.05	-0.08
inx-10	-0.26	0.23	0.55	-0.04	-0.40	0.31	-0.21	0.08	0.96	0.27	0.55	0.02	-0.01	0.04	0.05	-0.08	-0.05	0.06
inx-11	0.47	0.55	0.00	0.23	-0.60	-0.49	-0.40	-0.05	0.08	0.82	0.00	-0.08	-0.09	0.08	0.08	-0.10	-0.04	0.03
inx-12	0.01	-0.04	0.23	0.37	0.11	-0.09	-0.04	0.04	-0.22	0.06	0.23	-0.01	-0.02	0.14	-0.35	-0.04	0.01	0.00
inx-13	-0.34	-0.40	-0.60	0.11	0.41	0.06	0.26	-0.01	-1.05	-0.23	-0.60	0.04	0.11	0.15	-0.19	0.00	0.07	-0.08
inx-17	0.37	0.31	-0.49	-0.09	0.06	0.09	-0.14	0.05	-0.11	-0.19	-0.49	-0.11	-0.14	-0.04	0.35	0.23	-0.05	0.03
inx-18	0.08	-0.21	-0.40	-0.04	0.26	-0.14	0.13	-0.04	-0.24	-0.08	-0.40	0.14	0.04	-0.01	-0.03	-0.03	0.06	-0.04
inx-19	-0.01	0.08	-0.05	0.04	-0.01	0.05	-0.04	0.09	0.02	0.04	-0.05	-0.03	-0.03	-0.03	0.01	0.04	0.01	-0.01
inx-2	0.07	0.96	0.08	-0.22	-1.05	-0.11	-0.24	0.02	1.93	0.60	0.08	-0.16	-0.34	-0.04	-0.05	0.20	0.00	0.21
inx-3	0.05	0.27	0.82	0.06	-0.23	-0.19	-0.08	0.04	0.60	0.51	0.82	-0.14	-0.16	0.00	-0.15	-0.10	-0.04	0.05
inx-5	0.47	0.55	0.00	0.23	-0.60	-0.49	-0.40	-0.05	0.08	0.82	0.00	-0.08	-0.09	0.08	0.08	-0.10	-0.04	0.03
inx-6	0.15	0.02	-0.08	-0.01	0.04	-0.11	0.14	-0.03	-0.16	-0.14	-0.08	0.11	0.01	0.03	-0.08	0.13	-0.01	0.00
inx-7	0.09	-0.01	-0.09	-0.02	0.11	-0.14	0.04	-0.03	-0.34	-0.16	-0.09	0.01	0.11	0.06	0.04	0.03	0.05	-0.05
inx-8	-0.37	0.04	0.08	0.14	0.15	-0.04	-0.01	-0.03	-0.04	0.00	0.08	0.03	0.06	0.07	-0.17	-0.01	-0.02	-0.01
inx-9	0.00	0.05	0.08	-0.35	-0.19	0.35	-0.03	0.01	-0.05	-0.15	0.08	-0.08	0.04	-0.17	0.52	-0.02	-0.02	-0.01
che-7	0.14	-0.08	-0.10	-0.04	0.00	0.23	-0.03	0.04	0.20	-0.10	-0.10	0.13	0.03	-0.01	-0.02	0.06	0.00	0.00
unc-7	0.05	-0.05	-0.04	0.01	0.07	-0.05	0.06	0.01	0.00	-0.04	-0.04	-0.01	0.05	-0.02	-0.02	0.00	0.04	-0.03
unc-9	-0.08	0.06	0.03	0.00	-0.08	0.03	-0.04	-0.01	0.21	0.05	0.03	0.00	-0.05	-0.01	-0.01	0.00	-0.03	0.07

Fig. S6. Solution of the SCM with the Moore-Penrose pseudoinverse, corrseponding to $\alpha \to 0$. Top: Cook et al. data. Bottom: Varshney et al. data.

References

1. Varshney LR, Chen BL, Paniagua E, Hall DH, Chklovskii DB (2011) Structural properties of the caenorhabditis elegans neuronal network. *PLoS computational biology* 7(2).
2. Cook SJ, et al. (2019) Whole-animal connectomes of both caenorhabditis elegans sexes. *Nature* 571(7763):63–71.
3. Simonsen K, Moerman D, Naus CC (2014) Gap junctions in c. elegans. *Frontiers in physiology* 5:40.
4. Carrillo RA, et al. (2015) Control of synaptic connectivity by a network of drosophila igsf cell surface proteins. *Cell* 163(7):1770–1782.